Romanian Reports in Physics, Vol. 60, No. 4, P. 947–955, 2008

Dedicated to Prof. Voicu Lupei's
70th Anniversary

EFFECTS OF PARTICLE SIZE ON THE LUMINESCENCE OF YVO_4:Eu NANOCRYSTALS

S. GEORGESCU, E. COTOI, A. M. VOICULESCU, O. TOMA

National Institute for Laser, Plasma and Radiation Physics, Solid State Quantum Electronics Laboratory, Magurele, P.O. Box MG-36, Romania

(Received August 1, 2008)

Abstract. YVO_4:Eu nanocrystals synthesized by direct precipitation reaction. The morphologic transformation of the nanocrystals as the results of thermal treatments were analyzed using optical spectroscopy. A red shift of the fluorescence lines with the increase of the crystallite size was observed. The kinetics of the $^5D_0$ level of Eu^{3+} is also analyzed.

Key words: nanocrystals, YVO_4, Eu^{3+}, luminescence, nephelauxetic effect, covalency.

1. INTRODUCTION

In recent years, rare-earth-doped nanocrystalline phosphors have attracted great interest. Among the various host materials researched, much attention has been given to YVO_4:Eu^{3+}, which was used as red phosphor in color television cathode ray tube displays and high pressure mercury lamps. Recent studies show that nanosized YVO_4:Eu has significant promise in plasma display panels (PDP) [1].

Different methods have been used to prepare YVO_4:Eu^{3+} since it was introduced by Levine and Pallia in 1964 [2], high temperature solid state method [3], hydrolyzed colloid reaction technique [4], hydrothermal methods [1, 5], precipitation techniques [6, 7], etc.

YVO_4 has the zircon structure (space group $I4_1/amd$, lattice parameters $a = 7.1183$ Å, $c = 6.2893$ Å [8]). The lanthanide ion substitutes for yttrium in the YVO_4 lattice. This site has D_{2d} symmetry.

The introduction of the rare earth ions in crystals results in two effects: splitting of the degenerate levels and shift of the gravity center of the levels. This last effect is related to the nephelauxetic effect [9] which is a measure of the metal-ligand covalency. The difference between the bulk crystals and the nanocrystals of various size concerning the neighborhood of the metal ion could modify the

splitting of the energy levels, the metal-ligand covalency and the kinetics of the metastable levels.

For nanocrystals doped with rare earth ions a valuable tool in the investigation of the morphology changes produced by various thermal treatments is the optical spectroscopy. In the case of Eu^{3+}, the luminescence line spectrum is relatively easy to analyze since the strongest transitions originate from an energy state ($^5D_0$) not split by the crystal field. Consequently, the Eu^{3+} ion has been extensively used to probe the local environment of dopant sites.

In the precedent papers [10, 11] we presented some results concerning the morphological transformations induced by the thermal treatments on the YVO_4 nanocrystals synthesized by coprecipitation. These transformations were monitored by optical (probe Eu^{3+}) and EPR spectroscopy (probe Gd^{3+}) [10] and by optical and Mössbauer techniques (probe Eu^{3+}) [11]. All these investigations put in evidence the improving of the order and the reduction of the surface influence as a result of the increase of the particle size as a result of the thermal treatments.

In this paper we present new data concerning the luminescence properties of YVO_4:Eu nanophosphors. The fluorescence spectroscopy was used to monitor the morphological transformations induced by the thermal treatments in YVO_4 nanocrystals synthesized by direct precipitation reaction. For comparison, microcrystalline powder (bulk material) of YVO_4:Eu was synthesized by the solid state reaction.

2. EXPERIMENTAL

YVO_4 nanocrystals were prepared by direct precipitation reaction [6]. Two solutions, $Y(NO_3)_3$ and $Eu(NO_3)_3$, were prepared and added to a solution of NH_4VO_3 adjusted to pH 12.5 with NaOH. The obtained colloid was heated at 60°C for one hour with magnetic stirring. The resulting nanocrystals of YVO_4:Eu^{3+} (5 at.%) were separated from the solution by filtering and then dried at 60°C. The nanopowders were annealed in air, at various temperatures (300°C, 400°C, 500°C, 550°C, 600°C, 700°C, 900°C and 1300°C), for 4 hours.

The microcrystalline YVO_4:Eu was synthesized by solid state reaction [12] using a Y_2O_3, Eu_2O_3 and NH_4VO_3 mixture. This mixture was fired at 1000°C for one hour, then powderised and fired again at 1200°C for one hour. The resulted powder was washed with a solution of NaOH in water, dried and fired at 1200°C for one hour.

The experimental apparatus used for optical fluorescence measurements consisted of a 1 m Jarrell-Ash monochromator equipped with an S-20 photo-multiplier and a SR 830 lock-in amplifier on line with a computer. Eu^{3+}

fluorescence was excited with a Xenon lamp equipped with suitable optical filters (pump transition: $^7F_0 \rightarrow {}^5L_6$). For the lifetime measurements, the europium luminescence was excited with the second harmonic of the Nd:YAG laser Solar II and analyzed with a TURBO MCS scaler on line with a computer.

All the measurements were performed at room temperature.

3. RESULTS AND DISCUSSION

The results of the XRD analysis on the YVO_4:Eu nanopowders were presented elsewhere [10]. The crystallite size (in fact, the coherence domain) varied between ~ 6 nm for the 'as prepared' sample and ~ 60 nm for the sample annealed at 900°C The dependence of the crystallite size function of the thermal treatment temperature presented three temperature domains: in the first domain (between 60°C and ~ 400°C) the size of the particle increased slowly; in the second (~ 400°C–700°C) a rapid size increase was observed; finally, in the third one (700°C–900°C) no noticeable increase of the particle size was present. These temperature domains reflect the dynamics of the increase of the nanoparticle size [10]: from 60 nm to 12 nm in the first domain, from 12 nm to 60 nm in the second and no noticeable modification in the third. In the present paper the domain of the thermal treatments was extended at 1300°C, but the corresponding XRD data are not yet available. Moreover, for comparison, we analyzed an YVO_4:Eu powder synthesized by solid state reaction (bulk material).

3.1. LUMINESCENCE SPECTRA

The luminescence spectra for three YVO_4:Eu samples (the 'as prepared', denoted 60°C), the sample annealed at 900°C as well as the bulk sample (prepared by solid state reaction) are given in Fig. 1. The fluorescence lines in the spectrum of the 'as prepared sample' are wide, denoting disorder near the Eu^{3+} ion. On the contrary, the fluorescence lines of the sample annealed at 900°C are narrow, close to the line of the bulk material. The dependence of the linewidth on the annealing temperature was discussed in [10].

In order to see if the position of the fluorescence lines changes as the result of the thermal treatments, since the $^5D_0 \rightarrow {}^7F_0$ transition is forbidden in D_{2d} symmetry, we analyzed in details the transition $^5D_0 \rightarrow {}^7F_1$. We have chosen this transition because all the lines are evidenced and the position of the center of gravity can be calculated. In the D_{2d} symmetry the level $^7F_1$ splits in two Stark components so that we observe only two lines in the spectrum: $^5D_0\ (A_1) \rightarrow {}^7F_1\ (A_2)$

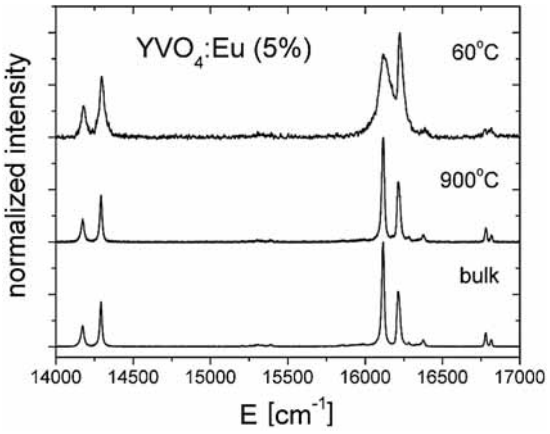

Fig. 1 – Fluorescence spectrum of three YVO_4:Eu (5%) samples: the 'as prepared' one (60°C), the sample annealed at 900°C, and the sample synthesized by solid state reaction (bulk).

and $^5D_0$ (A_1) $\rightarrow$ $^7F_1$ (E) [13]. A_1 and A_2 represent no degenerate representation of the group D_{2d} while E represents a doubly degenerate one.

Since we are interested in the shift of the gravity center of the $^7F_1$ level, we calculated the position of the gravity center of the transition:

$$E_c = \frac{2E_2 + E_1}{3}, \tag{1}$$

where E_1 is the position of the line corresponding to $^5D_0$ (A_1) $\rightarrow$ $^7F_1$ (A_2) and E_2 to $^5D_0$ (A_1) $\rightarrow$ $^7F_1$ (E). According to [13], $E_2 < E_1$. The results are given in Fig. 2.

The dependence of the position of the center of gravity of $^5D_0 \rightarrow {}^7F_1$ transition on the annealing temperature is not monotonous. The 'red shift' reaches its maximum (approx. 10 cm^{-1} in rapport with the value measured in the 'as prepared' sample) for 550°C. The significance of this maximum in not clear in present.

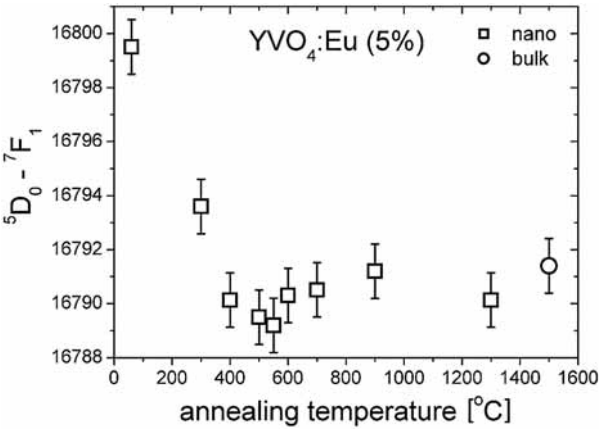

Fig. 2 – Squares: the red shift of the gravity center of the $^5D_0 \rightarrow {}^7F_1$ transition in YVO_4:Eu (5%) nanocrystals function of the annealing temperature. Circle: for comparison, the position of the gravity center of $^5D_0 \rightarrow {}^7F_1$ transition in YVO_4:Eu (5%) bulk is shown.

The red shift of the fluorescence lines with the annealing temperature is observed for other transitions too. For example, in Fig. 3, we show the dependence of the position of the most intense two lines belonging to the $^5D_0 \rightarrow {}^7F_4$ transition: $^5D_0$ (A_1) $\rightarrow {}^7F_4$ ($E^{(1)}$) and $^5D_0$ (A_1) $\rightarrow {}^7F_4$ (B_2) according to [13]. Because not all the lines of this transition can be separated in the fluorescence spectrum, we can not calculate the position of the gravity center.

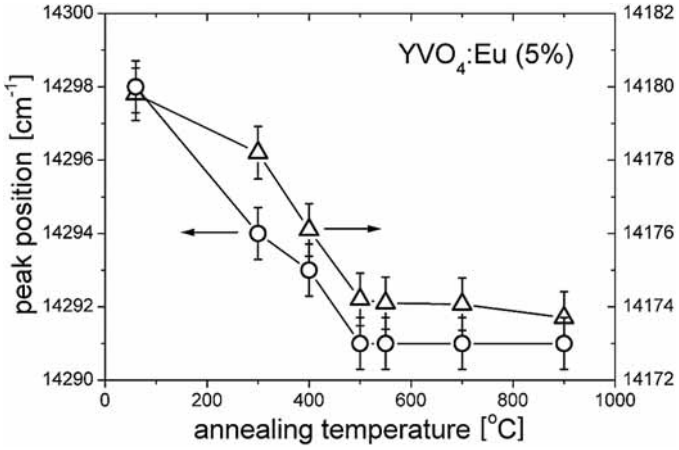

Fig. 3 – The red shift of the most intense two fluorescence lines belonging to the $^5D_0 \rightarrow {}^7F_4$ transition.

The red shift of the emission lines is a consequence of the nephelauxetic effect [9]. If a lanthanide ion is embedded in a crystal, the 4f electron clouds expand, and the Slater parameters F_k and the spin-orbit parameter ζ decrease. As a result, all the distances between the energy levels decrease and the absorption and the luminescence lines are red shifted in rapport with the free ion. The nephelauxetic effect was related to the covalency of the metal-ligand [9]. Therefore, increasing the thermal treatment temperature (resulting in the increase of the nanoparticle size) the covalency of the Eu^{3+} - O^{2-} bonds in YVO_4:Eu increases. According to Figs. 2, 3, this effect can be observed for the samples annealed up to ~ 550°C, *i.e.* for crystallite size up to ~ 30 nm (coherence domain).

The increase of the covalency with the nanoparticle size could be related with the expansion of the cell parameters of YVO_4 nanoparticles in rapport with the bulk material. Though there are not (in our best knowledge) such published data for YVO_4 nanoparticles, we could still consider the existence of this expansion in analogy with other oxides nanoparticles [14–16]. Thus, we could relate the observed increase of the covalency with the reduction of the Eu^{3+} - O^{2-} distance due to the thermal treatments.

3.2. KINETICS OF LUMINESCENCE

We analyzed the luminescence kinetics of the $^5D_0$ level in the YVO_4:Eu nanopowders annealed at temperatures up to 1300°C and in the bulk sample. The luminescence was excited with the second harmonic of the Nd:YAG laser (532 nm, pump transition is $^7F_1 \rightarrow {}^5D_1$). The kinetics is generally non-exponential except for the sample annealed at 1300°C and the bulk sample. The risetime observed for all the samples is due to the kinetics of the $^5D_1$ level of Eu^{3+}. A value of ~ 6.5 μs was obtained for the risetime ($^5D_1$ lifetime), in concordance with Ref. [17].

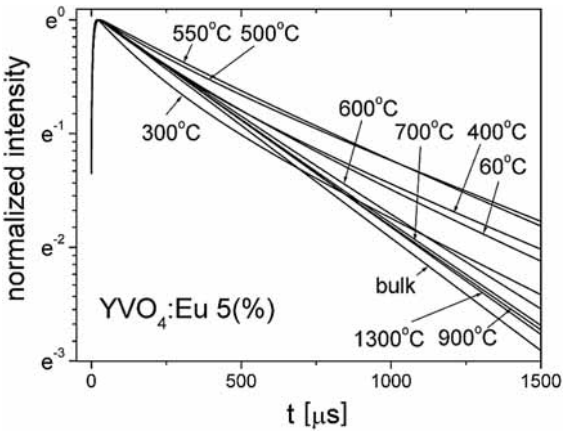

Fig. 4 – Semi logarithmic plot of the decay of $^5D_0$ level in YVO_4:Eu nanopowders annealed at various temperatures. The decay in the bulk sample is also shown.

Increasing the annealing temperature the decays becomes closer to exponential.

In order to compare the nonexponential decays we calculated an effective lifetime as the area of the normalized decay. For an exponential decay, in absence of risetime, this effective value is exactly the lifetime. The results are shown in Fig. 5.

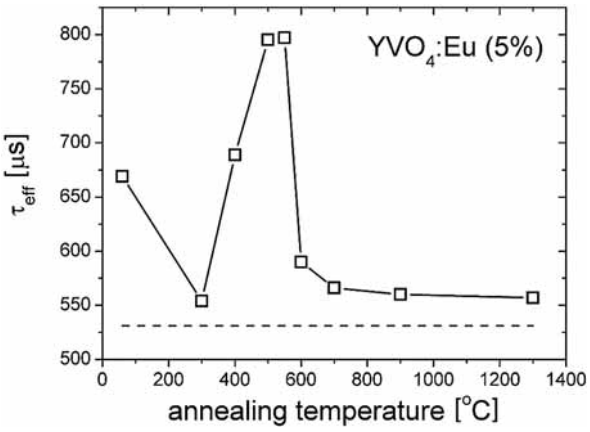

Fig. 5 – Dependence of the effective lifetime of the annealing temperature. Dotted line represents the effective lifetime of the bulk sample.

The fluorescence (observed) lifetime τ_{fl} depends on the radiative (characterized by the radiative lifetime τ_r) and nonradiative de-excitation processes (transition probability A_{nr}):

$$\frac{1}{\tau_{fl}} = \frac{1}{\tau_r} + A_{nr}. \tag{2}$$

There are two main factors which influence the decay of $^5D_0$ level of Eu^{3+} in nanocrystals: transfer to impurities adsorbed at the nanoparticle surface (nonradiative processes) and the effective index of refraction. When the size of the nanocrystallites is much less the radiation wavelength, the radiation 'feels' an effective index of refraction which is an average between the index of refraction of the crystallite and that of the surrounding medium [18].

For an electric-dipole transition the radiative lifetime is

$$\tau_r = \frac{1}{f(ED)} \frac{\lambda_0^2}{\left[\frac{1}{3}\left(n^2+2\right)\right]^2 n}, \tag{3}$$

where $f(ED)$ is the oscillator strength, λ_0 is wavelength in vacuum and n is the refractive index. Because the nanoparticles occupy only a small fraction x of the volume, we can define an effective refraction index

$$n_{eff}(x) = x\, n_{YVO_4} + (1-x)\, n_{air}, \tag{4}$$

$n_{YVO_4} \approx 2$ and $n_{air} \approx 1$, being the indexes of refraction. The reduction of the effective refractive index in rapport with the bulk material increases the radiative lifetime and, as a result, the fluorescence lifetime. On the contrary, the transfer to impurities increases the nonradiative transition probability A_{nr}, leading to the reduction of the fluorescence lifetime.

Both effects can be observed in the decay of $^5D_0$ level in YVO_4:Eu nanocrystals.

The energy gap between Eu^{3+} level $^5D_0$ and $^7F_6$ is quite large ~ 12000 cm^{-1}. This corresponds approximately to the third harmonic of the OH^- oscillator [19]. Therefore, OH^- is a very efficient quencher of Eu^{3+} emission and is present at the nanoparticle surface as a result of the wet synthesis. The thermal treatments remove the adsorbed OH^- and other impurities from the nanoparticle surface, resulting an increase of the fluorescent lifetime.

The radiative lifetime depends on the effective refractive index which, in turn, depends on the fraction of the volume occupied by the nanocrystals. This volume fraction depends on the agglomeration of the nanoparticles. The agglomerate size decreases with increasing temperature [20]. Therefore, there is no simple dependence of the effective refractive index of the annealing temperature.

Since the two main factors which influence the kinetics of the $^5D_0$ luminescence manifest an opposite tendency with annealing temperature we may expect a maximal value of the fluorescence lifetime. This is observed in the temperature interval 500°C–550°C. For higher temperatures, though the number of the surface quenchers is reduced, the increase of the nanoparticle size increases the effective refraction index, reducing the radiative lifetime.

A special behavior is observed for the sample annealed at 300°C (Figs. 4 and 5). The shape of the decay at few hundreds of microseconds after the beginning (Fig. 4) could be interpreted as very efficient transfer to impurities. For the time being, this behavior is not clear to us and needs supplementary investigations.

4. CONCLUSIONS

The YVO_4:Eu nanocrystals were synthesized by direct precipitation reaction. The size of the 'as prepared' nanocrystallites is ~ 6 nm (coherence domain for XRD). As a result of thermal treatments, the crystallite size increases (~ 60 nm for thermal treatment at 900°C).

The morphological transformations of the nanocrystallites due to the thermal treatments are monitorized using optical spectroscopy, sensitive probe being Eu^{3+}.

For YVO_4:Eu nanocrystallites smaller than ~ 30 nm a significant red shift of the fluorescence lines is noted. In analogy with other oxides, we related this shift with the increasing covalency due the possible reduction of the Eu^{3+} - O^{2-} as the crystallite dimensions increase due to the thermal treatments.

The kinetics of the $^5D_0$ level was affected by two main processes: transfer to impurities present at the particle surface and the modification of the radiative transition probability due to the 'effective' index of refraction – an average between the index of refraction of the crystallite and the index of refraction of the surrounding air. The fluorescence lifetime presents a maximal value for the samples annealed at 500°C–550°C. For higher annealing temperatures the decay becomes shorter and closer to exponential.

REFERENCES

1. K. Riwotzki, M. Haase, *Wet-Chemical Synthesis of Doped Colloidal Nanoparticles: YVO_4: Ln (Ln = Eu, Sm, Dy)*, J. Phys. Chem., B **102**, 10129–10135 (1998).
2. A. K. Levine, F. C. Palilla, *A new, highly efficient red-emitting cathodoluminescent phosphor (YVO_4:Eu) for color television*, Appl. Phys. Lett., **5**, 118–120 (1964).
3. R. C. Ropp, *Spectra of Some Rare Earth Vanadates*, J. Electrochem. Soc., **115**, 940–945 (1968).
4. S. Erdei, *Preparation of YVO_4 powder from the Y_2O_3 + V_2O_5 + H_2O system by a hydrolyzed colloid reaction (HCR) technique*, J. Mater. Sci., **30**, 4950–4959 (1995).

5. H. Wu, H. Xu, Q. Su, T. Chen, M. Wu, *Size- and shape-tailored hydrothermal synthesis of YVO_4 crystals in ultra-wide pH range conditions*, J. Mater. Chem., **13**, 1223–1228 (2003).
6. Y. Li, G. Hong, *Synthesis and luminescence properties of nanocrystalline $YVO_4:Eu^{3+}$*, J. Sol. State Chem., **178**, 645–649 (2005).
7. A. Newport, J. Silver, A. Vecht, *The synthesis of fine particle yttrium vanadate phosphors from spherical powder precursors using urea precipitation*, J. Electrochem. Soc., **147**, 3944–3947 (2000).
8. B. C. Chakoumakos, M. M. Abraham, L. A. Boatner, *Crystal structure refinements of zircon type MVO_4 (M = Sc, Y, Ce, Pr, Nd, Tb, Ho, Er, Tm, Yb, Lu)*, J. Solid State Chem., **109**, 197–202 (1994).
9. C. K. Jørgensen, *Modern Aspects of Ligand Field Theory*, North-Holland, Amsterdam, 1971.
10. S. Georgescu, E. Cotoi, A. M. Voiculescu, O. Toma, M. N. Grecu, E. Borca, S. Hodorogea, *Optical spectroscopy and EPR investigation of the thermal treatment effects on YVO_4 nanocrystal*, submitted to J. Optoelectron. Adv. Mater.
11. A. M. Voiculescu, E. Cotoi, O. Toma, S. Georgescu, S. Constantinescu, I. Bibicu, *Optical and Mössbauer spectroscopy studies on YVO_4:Eu nanophosphor*, submitted to J. Optoelectron. Adv. Mater.
12. W. M. Yen, M. J. Weber, *Inorganic phosphors: compositions, preparations, and optical properties*, CRC Press, 2004.
13. C. Brecher, H. Samelson, A. Lempicki, R. Riley, T. Peters, *Polarized spectra and crystal-field parameters of Eu^{3+} in YVO_4*, Phys. Rev., **155**, 178–187 (1967).
14. T. C. Huang, M. T. Wang, H. S. Sheu, W. F. Hsieh, *Size-dependent lattice dynamics of barium titanate nanoparticles*, J. Phys.: Condens. Matter, **19,** 476212 (2007).
15. V. Swamy, D. Menzies, B. C. Muddle, A. Kuznetsov, L. S. Dubrovinsky, Q. Dai, V. Dmitriev, *Nonlinear size dependence of anatase TiO_2 lattice parameters*, Appl. Phys. Lett., **88**, 243103 (2006).
16. D. Hreniak, J. Hölsä, M. Lastusaari, W. Stręk, *Effect of grain size and concentration of active ions on structural and optical behavior of Eu^{3+}-doped $Y_3Al_5O_{12}$ nanocrystallites*, J. Lumin., **122–123**, 91–94 (2007).
17. K. Riwotzki, *Synthese und optische Untersuchung seltenerd-dotierter, lumineszierender Nanokristallite* (in German), PhD Thesis, Hamburg University, 2001.
18. R. S. Meltzer, S. P. Feofilov, B. Tissue, H. B. Yuan, *Dependence of fluorescence lifetimes of $Y_2O_3:Eu^{3+}$ nanoparticles on the surrounding medium*, Phys. Rev., B **60**, R14012–R14015 (1999).
19. A. Huignard, V. Buissette, A.-C. Franville, T. Gacoin, J.-P. Boilot, *Emission processes in YVO_4:Eu nanoparticles*, J. Phys. Chem. B, **107**, 6754–6759 (2003).
20. J. A. Nelson, E. L. Brant, M. J. Wagner, *Nanocrystalline Y_2O_3:Eu phosphors prepared by alkalide reduction*, Chem. Mater., **15**, 688–693 (2003).